ASTROBIOLOGY
Volume 15, Number 4, 2015

DOI: 10.1089/ast.2014.1242

Purification, Biochemical Characterization, and Implications of an Alkali-Tolerant Catalase from the Spacecraft-Associated and Oxidation-Resistant *Acinetobacter gyllenbergii* 2P01AA

N. Muster, I. Derecho, F. Dallal, R. Alvarez, K.B. McCoy, and R. Mogul

Abstract

Herein, we report on the purification, characterization, and sequencing of catalase from *Acinetobacter gyllenbergii* 2P01AA, an extremely oxidation-resistant bacterium that was isolated from the Mars Phoenix spacecraft assembly facility. The *Acinetobacter* are dominant members of the microbial communities that inhabit spacecraft assembly facilities and consequently may serve as forward contaminants that could impact the integrity of future life-detection missions. Catalase was purified by using a 3-step chromatographic procedure, where mass spectrometry provided respective subunit and intact masses of 57.8 and 234.6 kDa, which were consistent with a small-subunit tetrameric catalase. Kinetics revealed an extreme pH stability with no loss in activity between pH 5 and 11.5 and provided respective k_{cat}/K_m and k_{cat} values of $\sim 10^7\ s^{-1}\ M^{-1}$ and $10^6\ s^{-1}$, which are among the highest reported for bacterial catalases. The amino acid sequence was deduced by in-depth peptide mapping, and structural homology suggested that the catalases from differing strains of *A. gyllenbergii* differ only at residues near the subunit interfaces, which may impact catalytic stability. Together, the kinetic, alkali-tolerant, and halotolerant properties of the catalase from *A. gyllenbergii* 2P01AA are significant, as they are consistent with molecular adaptations toward the alkaline, low-humidity, and potentially oxidizing conditions of spacecraft assembly facilities. Therefore, these results support the hypothesis that the selective pressures of the assembly facilities impact the microbial communities at the molecular level, which may have broad implications for future life-detection missions. Key Words: Catalase—Kinetics—Sequence—Stability—*Acinetobacter*—Spacecraft—Planetary protection. Astrobiology 15, 291–300.

1. Introduction

The *Acinetobacter* are potential microbial forward contaminants (Derecho *et al.*, 2014) that may impact the integrity of future life-detection missions on Mars (Space Studies Board, 2006). Molecular and cultivation studies show that the *Acinetobacter* are among the dominant members of the microbial communities that inhabit spacecraft and the associated assembly facilities (La Duc *et al.*, 2003, 2012; Ghosh *et al.*, 2010; Vaishampayan *et al.*, 2010). Hence, these microorganisms carry a high relative potential to be transported along with assembled spacecraft and serve as sources of false-positive signals of life. Crucially, molecular community analyses conducted during the Mars Phoenix lander assembly (Ghosh *et al.*, 2010; Vaishampayan *et al.*, 2010) indicated that the *Acinetobacter* possess tolerances toward (and potentially proliferate under) the assembly conditions despite the strict cleaning regimes, which included surface wiping with isopropanol and floor cleansing with alkaline detergents (Frick *et al.*, 2014). Specifically, these studies show that the operational taxonomic units (OTUs) associated with the *Acinetobacter* increased by ~9-fold throughout the assembly process, whereas, in contrast, the overall OTUs that represent the total bioburden decreased by ~3-fold (Vaishampayan *et al.*, 2010). Hence, these combined studies suggest that non-spore-forming bacteria such as the *Acinetobacter* may pose cleanliness issues for future life-detection missions.

The *Acinetobacter* are broadly associated with soil, water, and clinical environments (Gerischer, 2008) and have now been isolated and genetically detected in multiple spacecraft-associated environments, including the assembly facilities for space telescopes (Moissl-Eichinger *et al.*, 2013), the

California State Polytechnic University, Pomona, California.

assembly facilities for Mars-destined spacecraft (La Duc *et al.*, 2012), on the surface of the preflight Mars Odyssey orbiter (La Duc *et al.*, 2003, 2004b), and on surfaces and in the drinking water of the International Space Station (Castro *et al.*, 2004; La Duc *et al.*, 2004a). Recently, we reported on the characterization of *Acinetobacter gyllenbergii* 2P01AA, which was isolated from the floor of the Mars Phoenix assembly facility. Our studies show that *A. gyllenbergii* 2P01AA displays an extremotolerance toward hydrogen peroxide (H_2O_2) that is perhaps the highest known among Gram-negative and non-spore-forming bacteria (no loss in 100 m*M* H_2O_2) (McCoy *et al.*, 2012; Derecho *et al.*, 2014). Biochemical analyses showed that the extremotolerance is related to the enzymatic degradation of hydro- and alkylperoxides, as well as proteomic factors associated with energy management, protein synthesis and folding, membrane transport, and nucleotide metabolism (Derecho *et al.*, 2014).

Accordingly, the role of catalase, which is an enzyme that degrades H_2O_2, has been shown to be a key factor in the extremotolerance of spacecraft-associated microorganisms. For example, studies on *A. gyllenbergii* 2P01AA reveal very high catalase specific activities (1800 ± 350 Units/mg) that are ~130% of that of *Deinococcus radiodurans* R1 and ~50% of that of *Vibrio rumoiensis* S-1^T (Derecho *et al.*, 2014), which are radiation-resistant bacteria (Daly, 2009) and oxidation-resistant bacteria (Yumoto *et al.*, 1999), respectively. In fact, relatively high catalase specific activities have been found in all tested spacecraft-associated *Acinetobacter*, including all floor isolates from the Mars Phoenix assembly facility and from *A. radioresistens* 50v1, which was isolated from the surface of the preflight Mars Odyssey spacecraft (McCoy *et al.*, 2012; Derecho *et al.*, 2014). Studies on *A. radioresistens* 50v1 reveal that the catalase specific activities are inducible and increase by ~50% upon exposure to 1 m*M* H_2O_2 (McCoy *et al.*, 2012). Further, catalases have been implicated in spore protection for the spacecraft-associated *Bacillus pumilus* SAFR-032 (Checinska *et al.*, 2012). Thus, when considered together, these studies suggest that catalase is an important biochemical determinant for survival in spacecraft assembly facilities.

In this study, therefore, we describe the purification, characterization, and sequencing of a catalase from *A. gyllenbergii* 2P01AA and examine the implications toward survival in the assembly facilities. To date, there remain very few reports that focus on the biochemical characterizations of spacecraft-associated microorganisms (Gioia *et al.*, 2007; Checinska *et al.*, 2012; McCoy *et al.*, 2012; Derecho *et al.*, 2014), which is significant, as these types of analyses will assist in the interpretation of life-based detection experiments, such as those planned for the upcoming NASA Mars 2020 and ESA ExoMars 2018 missions. Hence, our current study represents the first reported purification and analysis of an enzyme from a spacecraft-associated microorganism. In summary, our results show that the catalase from *A. gyllenbergii* 2P01AA is extremely pH stable, alkali-tolerant, halotolerant, and possesses k_{cat}/K_m and k_{cat} values that are among the highest reported for bacterial catalases. Together, these properties are consistent with adaptations toward the alkaline, low-humidity, and potentially oxidizing conditions of spacecraft assembly facilities, and hence support the hypothesis that the assembly conditions impact the microorganisms at the molecular level.

2. Materials and Methods

2.1. Materials

Materials included Bugbuster Master Mix (EMD4Biosciences), Halt* Protease Inhibitor Cocktail (Thermo Scientific), bovine liver catalase (Calbiochem), sodium pyrophosphate (Sigma-Aldrich), HEPES (4-(2-hydroxyethyl)-1-piperazineethanesulfonic acid) (VWR), NaCl (VWR), phosphate-buffered saline (PBS; 10× PBS: 100 m*M* potassium phosphate, 100 m*M* NaCl, pH 7.4) (VWR), and 1 cm disposable BRAND semi-micro UV-cuvettes (VWR). Nonstabilized 30% w/w hydrogen peroxide (Sigma-Aldrich) was utilized in the kinetic reactions to eliminate the impacts of the stabilizers (*e.g.*, phenol, acetanilide, and sodium stanate); hydrogen peroxide solutions were stored as aliquots at −20°C. Lysogeny broth (LB) was prepared (per liter) by using 5.0 g of yeast extract (Becton Dickinson), 10.0 g of tryptone (Becton Dickinson), and 10.0 g of NaCl. All media were autoclaved at 121°C for 30 min, buffers and solutions were sterile filtered (0.22 μm), and pure water (18 MΩ cm^{-1}) was used throughout.

2.2. Catalase purification

Cultures of *Acinetobacter gyllenbergii* 2P01AA were prepared from glycerol stocks by streaking onto LB agar plates. After incubation overnight at 32°C, isolated colonies were cultivated to stationary phase (OD_{600} ~ 3.5) in LB at 32°C at 200 rpm (New Brunswick Scientific Innova 4200 incubator). A 1:100 inoculum of this culture was then used to prepare mid-log phase cultures (OD_{600} ~ 1.5) that were collected by centrifugation at 5445*g* at 4°C for 10 min (Beckman Allegra 21R centrifuge), washed three times in PBS [or 50 m*M* HEPES (pH 7.5) containing 100 m*M* NaCl], and stored as cell pellets at −80°C. Native catalase was purified from *A. gyllenbergii* 2P01AA by a 3-step chromatographic procedure on a Bio-Rad DuoFlow 10 chromatography system, which was equipped with a conductivity monitor and UV optics module. Cell pellets were partially thawed, resuspended in Bugbuster (5 mL per gram of wet pellet), mixed with Protease Inhibitor Cocktail (10 μL per 1 mL), and incubated at 22°C for 20 min. The suspension was clarified by centrifugation (5445*g* for 20 min at 4°C), the supernatant collected, and the soluble extract (~33.5 mL) was loaded at 5 mL/min onto a Bio-Rad UnoQ1 (1.5×11.3 cm) anion exchange column, which was equilibrated with 50 m*M* HEPES (pH 8.0). Elutions were performed at 5 mL/min with a NaCl step gradient in 50 m*M* HEPES (pH 8.0), which increased by 0.1 *M* NaCl every 25 mL from 0.2 to 0.8 *M* NaCl. Catalase activities (measured as described below) were detected in fractions eluting at ~24 mS/cm; these fractions were pooled and sequentially buffer exchanged and concentrated to 5–10 mL in 50 m*M* HEPES (pH 8.0) with an Amicon 10 kD Ultra-15 Centrifugal Device (VWR). The concentrated sample was subjected to size-exclusion chromatography (SEC) by using a Hi-Prep Sephacryl S-300 High Resolution column (1.6×60 cm), running buffer of 50 m*M* HEPES (pH 8.0), and flow rate of 1 mL/min. The catalase-active fractions were pooled, adjusted to 1 *M* NaCl, and separated by hydrophobic interaction chromatography (HIC) with a Phenyl Sepharose 6 Fast Flow column (1.6×10 cm), which was equilibrated in 50 m*M* HEPES (pH 8.0) containing 1 *M*

NaCl. Elution was performed at 1 mL/min by using a step gradient of 50 m*M* HEPES (pH 8.0), which decreased by 0.1 *M* NaCl every 35 mL. In sum, catalase activities were detected in the early fractions after SEC and in the fractions eluting between 0 and 0.1 *M* NaCl after HIC. Samples from each step in the purification were then analyzed by using 10% SDS-PAGE gels (Pierce Precise), which were run at 150 V for ~35 min (Bio-Rad Mini-Protean System), stained with Coomassie G-250, and quantified by densitometry (UnScan-It, Silk Scientific, Inc.).

2.3. Mass spectroscopy

Mass spectrometry was used to identify and characterize the catalase during and after the purification. Partially purified samples were separated on 10% SDS-PAGE gels, and a band corresponding to ~60 kDa was excised, subjected to in-gel trypsin digestion, and mass spectra of the products obtained on an Applied Biosystems 4800 MALDI/TOF mass spectrometer under MS and MS/MS modes (Institute for Integrated Research on Materials, Environment and Society, California State University, Long Beach). Spectra were assigned to bacterial sequences in the MSDB database by using 95% confidence intervals and the Mascot search engine (Matrix Science, Boston, MA). Upon purification, the amino acid sequence, intact molecular weight, subunit molecular weight, and ligand content were assessed. The catalase amino acid sequence was determined by liquid chromatography–tandem mass spectrometry (LC-MS/MS) analyses (Agilent capillary HPLC, Thermo LTQ-FT Ultra mass spectrometer) on differing proteolytic digests. To obtain maximum coverage, several proteolytic reagents were used, including trypsin (Roche), LysC (Roche), GluC (Roche), subtilisin (Sigma-Aldrich), chymotrypsin (Roche), and formic acid for chemical lysis (EMD). In general, the digestion procedures included concentration of the sample to >50 μg/mL, buffer exchange into 100 m*M* Tris-HCl (pH 8.0), addition of 0.1% RapiGest (Waters), and incubation at 99°C for 10 min. Upon conclusion and after cooling to room temperature (RT), 10 m*M* TCEP (Pierce) was added to the sample, incubated at RT for 30 min, after which 10 m*M* iodoacetamide (Sigma-Aldrich) was added, and the mixture incubated again for another 30 min at RT. Proteolytic enzymes (0.25–2 mg/mL) were then added to aliquots of the sample, incubated at 50°C for 1 h (25°C for chymotrypsin), and quenched by incubation in 0.1 *M* HCl at 37°C for 45 min. For the chemical lysis reactions, samples were incubated in 2% formic acid at 99°C for 120 min. The digests were then subjected to LC-MS/MS, and all spectra were matched to the NSCInr database with the MASCOT search engine and ≥95% confidence intervals. Gaps in the coverage were treated by using error-tolerant searches, manual inspection of the raw spectral data, and sequence homology to catalases from other *Acinetobacter* (≥95% identity). In the homology alignments, amino acid identities were tentatively assigned only when 100% homology was observed across the aligned strains. The mass of the intact catalase was obtained on a traveling wave ion mobility quadrupole time-of-flight mass spectrometer (Waters Q-TOF Synapt G2 mass spectrometer) by using >250 μg/mL samples, which had been buffer exchanged into 100 m*M* NH_4OAc (pH 7.0) overnight at 4°C with a 7000 MWCO mini dialysis unit (Thermo-Pierce). Mass of the catalase subunit was obtained under denaturing conditions by using >50 μg/mL samples and a time-of-flight mass spectrometer coupled to a nano-UPLC system equipped with a C18 nanospray column (Q-TOF Ultima & nanoAcquity; Waters, Milford, MA).

2.4. Absorption spectroscopy

Absorption spectra for the purified catalase were obtained with a Beckman Coulter DU-640 spectrophotometer. Spectra (240–800 nm) were acquired by using 16 μg/mL or 68 n*M* catalase in the absence and presence of 0.83 m*M* NaCN, where the mixtures were incubated for 10 min at 22°C prior to analysis.

2.5. Enzyme kinetics and inhibition

Enzyme kinetic studies on the purified catalase were performed by spectrally following the decomposition of H_2O_2 at 240 nm ($\varepsilon = 43.6\ M^{-1}\ cm^{-1}$). The change in absorbance was measured every 2 s, for a minimum of 30 s, on a Beckman Coulter DU- 640 spectrophotometer. All reactions were 1.00 mL in volume, run at RT (~22°C), and thoroughly but gently mixed. Reaction rates were measured between 5 and 100 m*M* H_2O_2 in 50 m*M* HEPES (pH 7.5) in absence and presence of 100 or 200 m*M* NaCl. Reactions were initiated by addition of enzyme by using a final concentration of 67 ng/mL or 0.29 n*M* catalase, which was calculated by using the intact molecular weight obtained from mass spectral studies and an assumption of full iron loading. Kinetic constants were obtained by using rates obtained between 10 and 50 m*M* H_2O_2, as regressions of the double-reciprocal plots within this concentration range provided coefficients of determination of $R^2 > 0.99$; the standard errors (*se*) of these regressions are reported herein. Inhibition studies were performed by using 3-amino-1,2,4-triazole (3AT), sodium azide (NaN_3), and sodium cyanide (NaCN). In summary, 6 μg/mL or 26 n*M* purified catalase was premixed with either 400 μM 3AT, 15 n*M* NaN_3, or 500 μM NaCN in 50 m*M* HEPES (pH 7.5), respectively. After incubation for 1 min at 22°C, the enzyme reaction rates were measured by using 60 ng/mL or 0.26 n*M* catalase and 20 m*M* H_2O_2 in 50 m*M* HEPES (pH 7.5). Control experiments on bovine liver catalase (BLC) were performed in parallel.

2.6. Temperature and pH stability profiles

Temperature stability profiles for catalase were obtained between the range of 10–100°C. Catalase samples (6 μg/mL or 26 n*M*) were incubated at 5–10°C increments for 15 min, equilibrated to RT over ~30 min, and assayed for enzymatic activity. Reaction conditions included 60 ng/mL or 0.26 n*M* catalase, 20 m*M* H_2O_2, and 50 m*M* HEPES buffer (pH 7.5) in absence and presence of 100 m*M* NaCl. The pH stability profiles for catalase were also obtained. Assay conditions included 60 ng/mL or 0.26 n*M* catalase, and 20 m*M* H_2O_2, in 30 m*M* sodium pyrophosphate adjusted to pH 2.5–11.5; control experiments indicated no change in the buffered pH upon conclusion of the kinetic reactions. All other conditions are as described.

3. Results

3.1. Catalase purification

The native catalase from the H_2O_2-resistant *Acinetobacter gyllenbergii* 2P01AA was purified by a 3-step

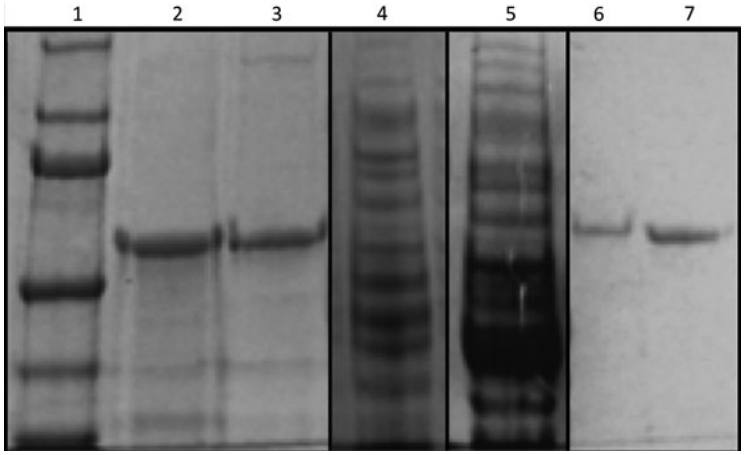

FIG. 1. Electrophoretic analysis (10% SDS-PAGE) of the catalase purification: Bio-Rad molecular weight standard (lane 1); BLC control (lane 2); purified and concentrated catalase from *A. gyllenbergii* 2P01AA (lane 3); catalase sample after anion exchange (lane 4); catalase sample after SEC (lane 5); catalase sample after hydrophobic interaction exchange (lane 6); and BLC control (lane 7).

chromatographic procedure following the order of anion exchange, SEC, and HIC (Fig. 1). As indicated in Table 1, the overall purification yield of the native catalase was 36%, which correlated to a $\sim$150-fold enrichment in specific activity to yield a final value of 8.7×10^6 Units/mg. Densitometry of the catalase samples separated by using 10% SDS-PAGE gels indicated a $>$95% purity after the 3-step procedure. Initial experiments showed that the order of separation was significant, as separations following the sequence of anion exchange, HIC, and SEC provided only $\sim$40% purity. The identity of the purified protein was confirmed as catalase by mass spectral analyses of trypsin digests of (A) a $\sim$60 kDa protein excised from electrophoretic gels during the purification, which provided matches to catalase from *Acinetobacter calcoaceticus* (Q83WC7_ACICA), and (B) the purified sample, which provided matches to *Acinetobacter junii* SH205 (D0SPS7).

3.2. Sequence and structural homology models

The amino acid sequence of catalase from *A. gyllenbergii* 2P01AA was determined through in-depth peptide mapping and the use of multiple proteolytic reagents, which ultimately provided 96% sequence coverage (Fig. 2). Error-tolerant searches of the mass spectra confirmed the identity of Ser^{385}, which corresponded to Gly in other *Acinetobacter*, and the constructed 1° structure revealed that the N-terminal methionine had been cleaved. BLAST comparisons in the NCBI database denoted a clade III catalase corresponding to the katE gene (von Ossowski *et al.*, 1991). Distance trees (NCBI) placed the catalase into a sub-branch of the *Acinetobacter* populated by *A. junii* and *A. gyllenbergii*, and indicated that the catalase was more closely related to *A. junii*, despite the confirmed taxonomy of the microorganism as *A. gyllenbergii*. The unassigned amino acids in the sequence (4% of the coverage) were assigned by sequence homology to catalases from 12 different species of *Acinetobacter*, where each catalase shared high identity values of $\geq$95% with the target sequence. At each position, the alignments showed 100% homology across all species with the exception of X^{274} (Fig. 2), which varied between Asp and Glu. For demonstrative purposes, alignments of the target sequence to *A. junii* SH205 (D0SPS7) and *A. gyllenbergii* MTCC 11365 (S3YMH9) are provided in Fig. 3A, which together aptly show the 100% homology at the unassigned positions. To remain consistent within the sequence analysis, the N-terminal amino acid for the purified catalase is assumed to be the cleaved methionine residue. Additionally, alignments across all known strains of *A. gyllenbergii*, as illustrated by the alignment to *A. gyllenbergii* MTCC 11365 (Fig. 3A), revealed several mutations that were unique to the 2P01AA strain. These mutations included V^{331} (A^{331} in *A. gyllenbergii* MTCC 11365), I^{379} (T^{379} in *A. gyllenbergii* MTCC 11365), Ser^{385} (G^{385} in *A. gyllenbergii* MTCC 11365), and the C-terminal residue of I^{506} (L^{506} in *A. gyllenbergii* MTCC 260 11365).

A structural homology model for catalase (Fig. 3B) was built by using the SWISS-MODEL template library (Arnold *et al.*, 2006; Benkert *et al.*, 2011; Biasini *et al.*, 2014), where BLAST and HHBlits searches of the target sequence identified the closest evolutionary related structure (from the Protein Data Bank) to be catalase (2isa) from *Vibrio salmonicida* (sequence identity, 74.16%). The ligand-free structural homology model displayed several aspects typical to small subunit catalases, including an intertwining N-terminal arm, an antiparallel eight-stranded β-barrel, and a

TABLE 1. CATALASE PURIFICATION YIELDS FROM *A. GYLLENBERGII* 2P01AA

Purification step	*Total protein (mg)*	*Total activity (Units)*	*Specific activity (Units/mg)*	*Purification fold*	*Yield (%)*
Crude extract	70	4.0×10^6	5.8×10^4	—	—
Anion exchange	8.0	2.2×10^6	2.7×10^5	4.7	54%
Size exclusion	3.0	2.0×10^6	6.9×10^5	12	49%
Hydrophobic interaction	0.17	1.4×10^6	8.7×10^6	150	36%

```
        10         20         30         40         50         60
MSQDDKKCPY SHLTTDFGAP VVDNQNSMTA GARGPLLAQD LWLNEKLANF VREVIPERRM
        70         80         90        100        110        120
HAKGSGAFGT FTVTHDITQY TRAKIFSEIG KKTEMFARFT TVAGERGAAD AERDIRGFAL
       130        140        150        160        170        180
KFYTEEGNWD MVGNNTPVFF LRDPRKFPDL NKAVKRDPKT NLRSATNNWD FWTLLPEALH
       190        200        210        220        230        240
QVTIVMSDRG IPASYRHMHG FSSHTYSFIN AANERFWVKF HFRTQQGIKN LTDAEAGELV
       250        260        270        280        290        300
GQDRESHQRD LFDAIERQDY PKWTLFVQIM PEQXAEKVPY HPFDLTKVWP HGDYPLIEVG
       310        320        330        340        350        360
EFELNRNSEN FFLDVEQSAF APSNLVPGIS VSPDRMLQAR LFNYADAQRY RLGVNYQQIP
       370        380        390        400        410        420
VNAARCPVHS NHRDGQGRID ANYGSLPHYE PNSFGQWQEQ PQYKEPPLKI NGDADFWDYR
       430        440        450        460        470        480
EDDNDYFSQP RALFELMTPE QQDALFGNTA RAMGDALDFI KYRHIRNCYA CHPAYGEGVA
       490        500
KALGMTVADA QAARETDPAR HLPSFI
```

FIG. 2. Amino acid sequence of catalase from *A. gyllenbergii* 2P01AA, where the residues identified by mass spectrometry are in bold font, while those assigned by homology are in nonbold font; the underlined amino acid (S^{385}) was confirmed with error-tolerant searches, X^{274} represents either Asp or Glu, the active site residues (His^{61}, Asn^{134}, Asn^{135}, Arg^{340}, and Tyr^{344}) are highlighted by boxes, and the sequence homology studies (UniProt) utilized alignments to catalases from *A. junii* MTCC 11364 (S7Y7D6), *A. junii* CIP 107470 (N9AZS1), *A. junii* SH205 (D0SPS7), *A. junii* CIP 64.5 (N9CBX8), *Acinetobacter* sp. NIPH 236 (N8R283), *Acinetobacter* sp. NIPH 284 (N9K5H2), *Acinetobacter* sp. NIPH 809 (N8QMK9), *A. gyllenbergii* MTCC 11365 (S3YMH9), *A. gyllenbergii* CIP 10306 (S3N7M0), *Acinetobacter* sp. ANC 3862 (N9N9I9), *A. gyllenbergii* NIPH 230 (V2TAZ6), and *Acinetobacter* sp. CIP 70.18 (N9RVW3).

C-terminal α-helical domain. Analysis of the structural model revealed that the mutations unique to the 2P01AA strain, among the known catalases from *A. gyllenbergii* (apart from the C-terminal residue), were all found at or near the interfaces between the catalase subunits, which may relate to the enhanced stability and kinetic properties. Further, Tyr^{344} was identified as the potential proximal Fe ligand, while His^{61}, Asn^{134}, and Arg^{340} comprised the major determinants of the active site. In summary, these results support the purification of a clade III catalase, which lacks an N-terminal methionine, contains a total of 505 amino acids per subunit, and displays a theoretical subunit pI of 5.81.

3.3. Mass and absorption spectroscopy

Mass spectrometry on the denatured sample provided a resolved mass of 57,813 Da for the catalase subunit, which is within experimental error of the theoretical molecular weight (57,796 Da, when including D^{274}). Further, analyses on the native samples provided a resolved mass of 234,613 Da for the intact catalase, which supported the purification of a catalase tetramer containing 4 Fe-heme (heme b) and 1–2 NADPH ligands per catalase. Absorption spectroscopy (Fig. 4) confirmed the presence of Fe-heme with a Soret band at 403 nm (molar absorptivity of $\sim 1.6\times10^{6}\ M^{-1}\ cm^{-1}$) and heme charge transfer bands at 502 and 625 nm (Deisseroth and Dounce, 1970; Obinger *et al.*, 1997; Thompson *et al.*, 2003). As shown in Fig. 4, the absorbance spectra were sensitive to the addition of cyanide, which yielded (A) a red shift in the λ_{max} of the Soret feature from 403 to 424 nm, (B) loss of peaks at 502 and 625 nm, and (C) the gain of the α- and β-peaks at 550 and 585 nm. Together, these features were consistent with conversion to a 6-coordinate low spin center upon cyanide ligation. Thus, the combined characterizations supported the purification of a Fe-heme-containing, small subunit, and tetrameric catalase with the native state possessing 5-coordinate high spin ferric centers.

3.4. Enzyme kinetics and inhibition

Kinetic studies on the catalase from *A. gyllenbergii* 2P01AA (Fig. 5) revealed significant substrate inhibition at concentrations of >50 m*M* H_2O_2 in 100 m*M* NaCl and >10 m*M* H_2O_2 in 200 m*M* NaCl [in 50 m*M* HEPES (pH 7.5)]. This non-Michaelis-Menten behavior is common to catalases and accordingly treated by including only lower H_2O_2 concentrations in the analyses (Switala and Loewen, 2002). Apparent kinetics constants were thus obtained by using the rates collected between 10 and 50 m*M* H_2O_2 in the absence and presence of 100 m*M* NaCl (Fig. 5). This analysis yielded an apparent K_m of 110 m*M* ($se = 29$ m*M*), which increased to 230 m*M* ($se = 110$ m*M*) in the presence of 100 m*M* NaCl [in 50 m*M* HEPES (pH 7.5)]. The V_{max} for catalase was $1.1\times10^{10}\ \mu M\ s^{-1}\ g^{-1}$ ($se = 0.3\times10^{10}\ \mu M\ s^{-1}\ g^{-1}$), which remained relatively constant in 100 m*M* NaCl at $1.2\times10^{10}\ \mu M\ s^{-1}\ g^{-1}$ ($se = 0.6\times10^{10}\ \mu M\ s^{-1}\ g^{-1}$). The corresponding apparent k_{cat} values were $2.5\times10^{6}\ s^{-1}$ ($se = 0.6\times10^{6}$) and $2.9\times10^{6}\ s^{-1}$ ($se = 1.4\times10^{6}$), respectively. Lastly, the apparent k_{cat}/K_m was $2.2\times10^{7}\ s^{-1}\ M^{-1}$ ($se = 0.09\times10^{7}$), which decreased to $1.2\times10^{7}\ s^{-1}\ M^{-1}$ ($se = 0.05\times10^{7}$) in 100 m*M* NaCl. Together, the parameters indicate that the presence of NaCl decreased the rate of substrate capture (k_{cat}/K_m) yet caused no significant impact on the rate of product release (k_{cat}) (Mogul and Holman, 2001). For demonstrative

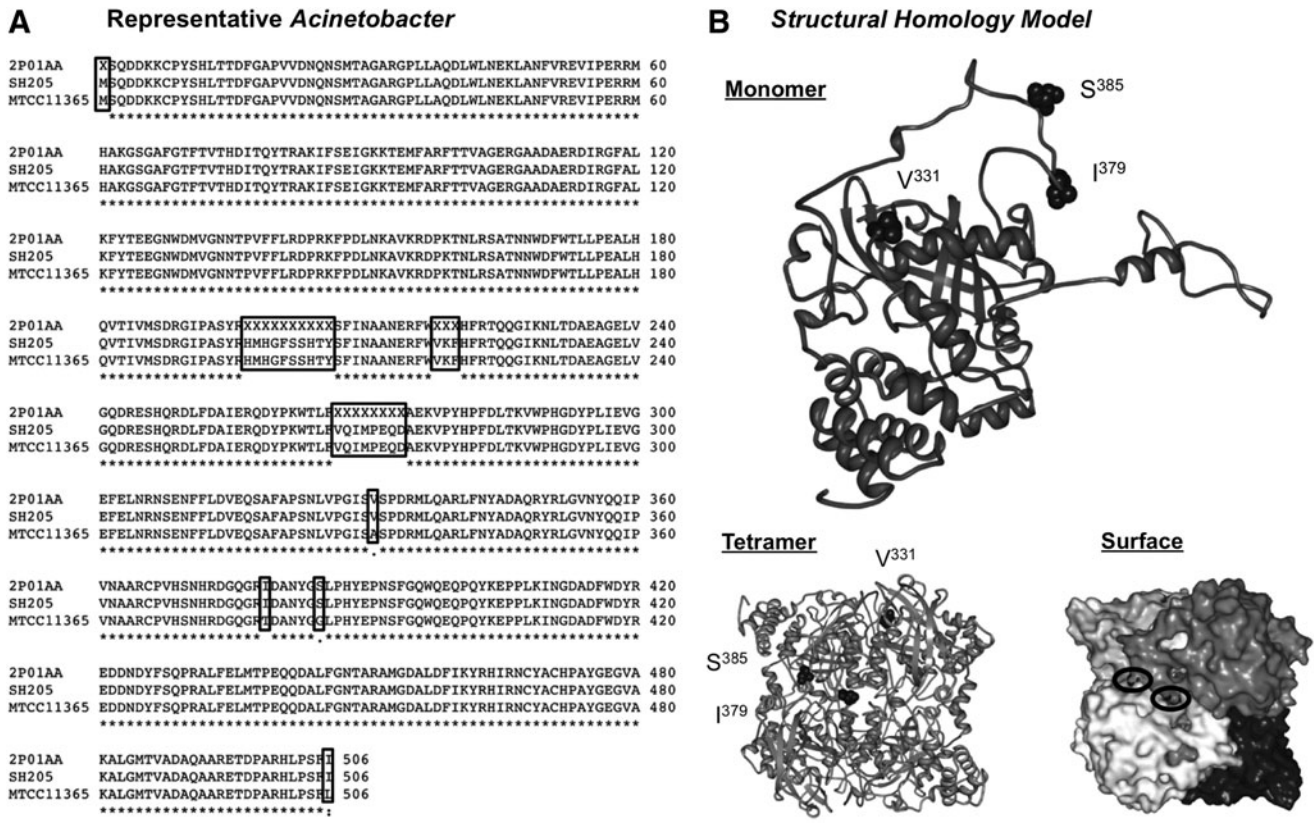

FIG. 3. Sequence and structural homology models for the catalase from *A. gyllenbergii* 2P01AA, where (**A**) the alignments (COBALT, NCBI) against the catalases from *A. junii* SH205 (D0SPS7) and *A. gyllenbergii* MTCC 11365 (S3YMH9) are signified by the respective abbreviations of 2P01AA, SH205, MTCC 11365; and (**B**) the structural homology models (SWISS-MODEL) of the catalase subunit, tetramer assembly, and surface view of the tetramer assembly display the relative positions of the residues (black, space-filling format, or ovals) that differ among the *A. gyllenbergii* strains. For the alignments, the unassigned amino acids are denoted by X, the asterisk demarcation (*) represents a fully conserved amino acid, the colon demarcation (:) represents conservation among the amino acid group, the period demarcation (.) represents conservation of the general amino acid property, and the boxes highlight the amino acids discussed in the narrative.

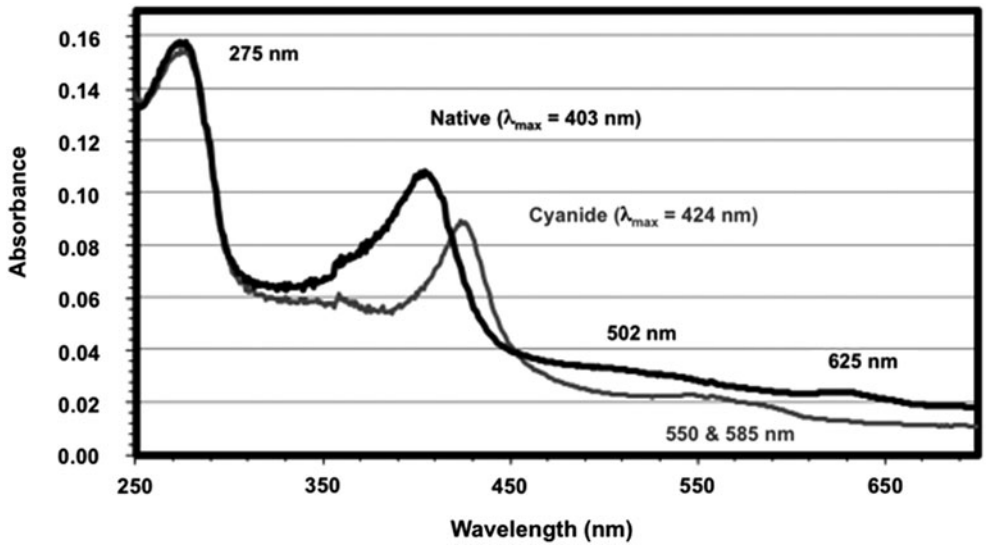

FIG. 4. Absorbance spectra of catalase from *A. gyllenbergii* 2P01AA in the absence (black line) and presence (gray line) of cyanide, where the impact of cyanide on the Soret bands (403 and 424 nm), heme charge transfer bands (502 and 625 nm), and α and β-bands (550 and 585 nm) are consistent with a native catalase that contains a 5-coordinate high spin ferric center.

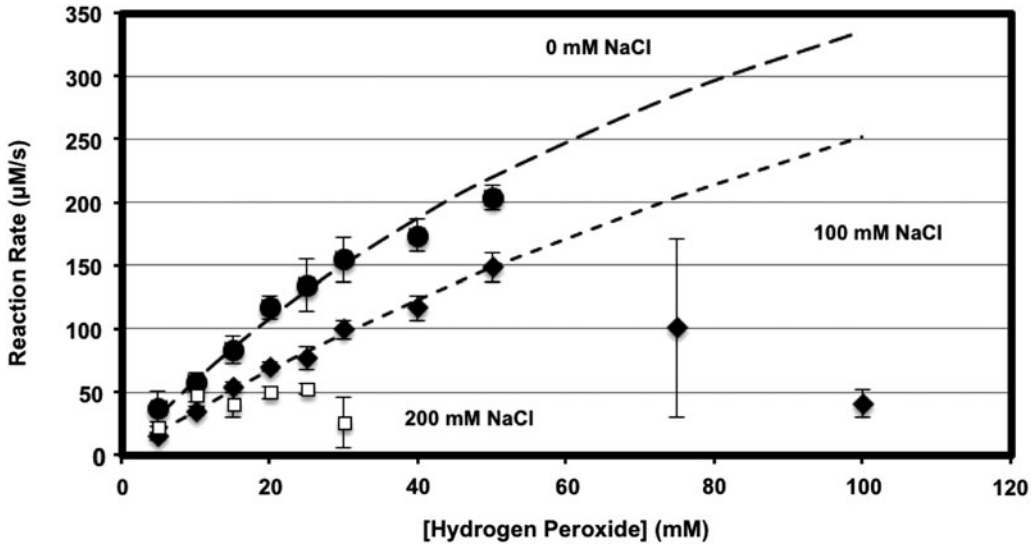

FIG. 5. Actual and theoretical impacts of H_2O_2 concentration on the rates of catalase, where the experimentally determined rates were obtained by using 5–100 m*M* H_2O_2 in 50 m*M* HEPES (pH 7.5) containing 0 (circles), 100 (diamonds), and 200 (squares) m*M* NaCl; the theoretical catalase rates (dashed lines) were calculated with the apparent kinetic constants and a Michaelis-Menten kinetic model, which excludes substrate inhibition (all rates were measured in triplicate, error bars represent the standard deviation, and all regressions were performed using coefficients of determination of ≥ 0.99).

purposes, the theoretical enzyme rates for catalase were calculated with the apparent kinetic constants and are displayed in Fig. 5. These comparisons of actual and theoretical rates effectively illustrate the pronounced substrate and solute inhibition by H_2O_2 and NaCl, respectively. Consequently, the rate data obtained in 200 m*M* NaCl could not be mathematically fitted due to significant substrate inhibition.

For control purposes, kinetic analyses were also performed on BLC. Under our conditions, significant substrate inhibition was observed at >25 m*M* H_2O_2; therefore, only the rates obtained between 10 and 20 m*M* H_2O were used in the kinetics. These analyses yielded apparent K_m values of 18 and 20 m*M* in the absence and presence of 100 m*M* NaCl, respectively. For comparative purposes, BLC was assumed to be fully loaded with iron; hence, an apparent k_{cat} of 7.4×10^4 s^{-1} was obtained, which decreased to 4.6×10^4 s^{-1} in 100 m*M* NaCl. The apparent k_{cat}/K_m was 3.6×10^6 s^{-1} M^{-1}, which decreased to 1.9×10^6 s^{-1} M^{-1} in 100 m*M* NaCl. Therefore, the presence of NaCl impacted both the rate of substrate capture and product release for BLC, which is in contrast to measured impact on the purified *Acinetobacter* catalase. Together, the impact of NaCl on the kinetics is consistent with a competitive-type inhibition by NaCl for the purified catalase, where increasing NaCl concentration correlates with an increasing K_m and relatively constant V_{max}. In comparison, the kinetics of BLC are consistent with noncompetitive inhibition, where increasing NaCl concentration correlates with a relatively constant K_m and decreasing V_{max}. However, these kinetic outcomes are most likely due to the impacts of ionic strength on the solution dynamics, protein structure, and protein ionization (Nakamura and Kimura, 1971; Loo and Erman, 1975; Luo *et al.*, 2004). Nevertheless, on average, as displayed in Fig. 6, NaCl reduced the rates of both enzymes by $51 \pm 4\%$ between 10 and 25 m*M* H_2O_2. However, at 30 m*M* H_2O_2, the rate of BLC was substantially decreased by $\sim 85\%$, whereas no change was observed for the catalase from the 2P01AA strain. Hence, when compared to BLC, the purified catalase possessed a greater tolerance toward substrate inhibition in 100 m*M* NaCl. This tolerance is further demonstrated by comparison of the rates in 200 m*M* NaCl, where no activity was measured for BLC. Lastly, inhibition studies in which 3AT, NaN_3, and NaCN were used showed $10.1 \pm 1.1\%$, $16.5 \pm 2.5\%$, and $88.4 \pm 1.1\%$ (standard deviation) reductions in rate, respectively.

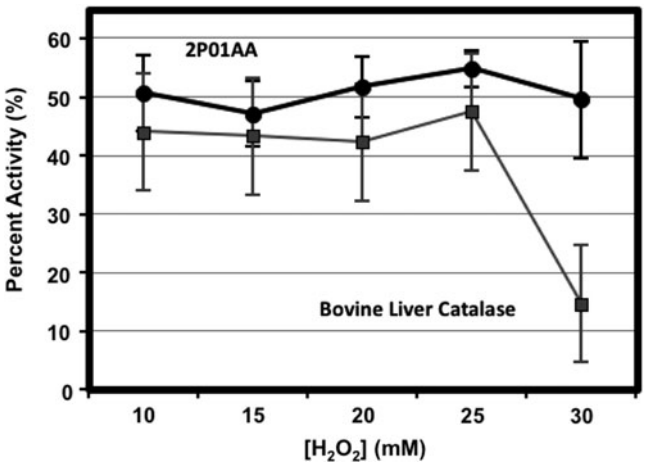

FIG. 6. Comparison of catalase inhibition by NaCl at differing concentrations of H_2O_2 for *A. gyllenbergii* 2P01AA (black marked line and circles) and BLC (gray marked line and squares), where the difference in rates measured in the absence (v_0) and presence (v_0^{NaCl}) of 100 m*M* NaCl between 10 and 30 m*M* H_2O_2 [in 50 m*M* HEPES (pH 7.5)] is expressed as a percent of the activity remaining after inhibition [Percent Activity $(\%) = (v_0^{NaCl}/v_0) \times 100$] (all rates were measured in triplicate, and error bars represent the standard deviation).

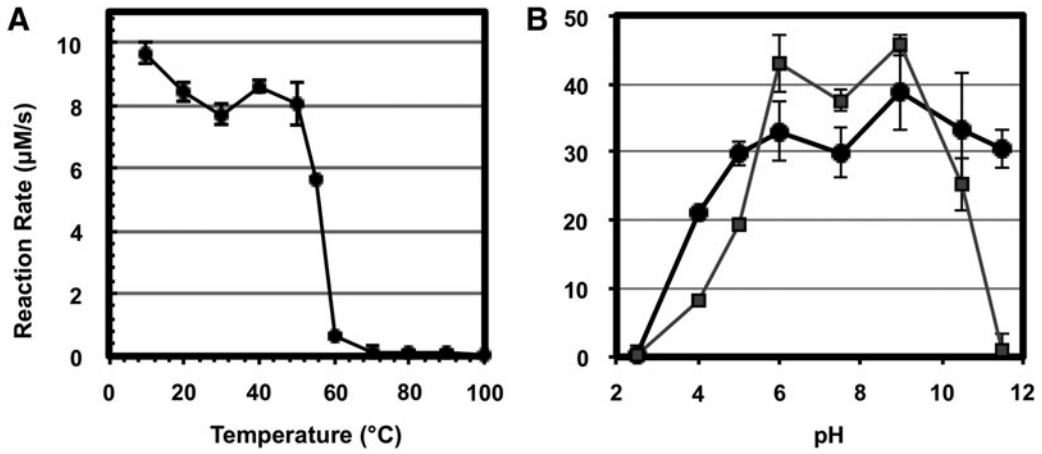

FIG. 7. Impacts of (**A**) temperature on catalase stability, which was assayed by measuring the change in catalase activity after 15 min incubations at the respective temperature, and (**B**) pH on catalase activity for *A. gyllenbergii* 2P01AA (black marked line and circles) and BLC (gray marked line and squares), where the activity assays were conducted by using 30 m*M* pyrophosphate buffers adjusted to pH values between 2.5 and 11.5 [assay conditions utilized 20 m*M* H_2O_2 in 50 m*M* HEPES (pH 7.5), all rates were measured in triplicate, and error bars represent the standard deviation].

3.5. Temperature and pH stability

Temperature and pH stability studies were conducted on catalase. Temperature stability provided an apparent T_m of 56°C and indicated that the catalase retained ~7% of the activity after incubation at 60°C for 15 min and that ≥70°C abolished all activity (Fig. 7A). Addition of NaCl had no major impact on the thermal stability of the enzymatic activity. The T_m for BLC has also been shown to be 56°C, with 100% deactivation occurring at ~62°C (Switala *et al.*, 1999). The catalase enzyme also was active from pH 4 to 11.5 and displayed a pH optimum of 5–11.5 (Fig. 7B), which is among the broadest pH optima for catalases (Esaka and Asahi, 1982; Allgood and Perry, 1986; Fu *et al.*, 2014). Notably, no loss in activity was measured between pH 5 and 11.5. However, at the more acidic values of pH 4 and 2.5, 50% and 100% losses in activity were obtained, respectively. In comparison, for BLC, the range in pH optima was 6–9, with significant losses at pH 5 (~55%) and pH 10.5 (~45%) and complete loss of activity at pH values of 2.5 and 11.5, respectively.

4. Discussion

Catalase from *Acinetobacter gyllenbergii* 2P01AA was purified with a 3-step chromatographic procedure, ultimately providing a 36% yield, final specific activity of 8.7×10^6 Units/mg, and purity of >95%. The resolved masses for the native catalase and denatured subunit were 234,613 and 57,813 Da, respectively, thereby supporting the purification of a tetramer catalase containing 4 Fe-heme b ligands. Absorbance spectra indicate that the Fe-heme groups were 5-coordinate high spin ferric centers. Sequence alignments indicate a clade III catalase with 505 amino acids per expressed and processed subunit, whereas the structural homology model suggests that mutations along the subunit interfaces were responsible for providing the unique stability and kinetic parameters among the catalases from differing strains of *A. gyllenbergii*. Kinetic studies provided an apparent K_m of 110 m*M*, which is similar to those displayed by catalases from *Helicobacter pylori, Listeria seeligeri, Saccharomyces cerevisiae* but ~2-fold lower than that of *Bacteroides fragilis* and *Serratia marcescens* and ~4-fold lower than that of *Aspergillus niger* and *Proteus mirabilis* (Switala and Loewen, 2002). Moreover, the respective k_{cat} and k_{cat}/K_m values of 2.5×10^6 s^{-1} and 2.2×10^7 s^{-1} M^{-1} are among the highest reported for bacterial catalases (Switala and Loewen, 2002; Thompson *et al.*, 2003).

Catalase was inhibited by 3AT, NaN_3, NaCN; displayed a competitive-type inhibition by NaCl; and was significantly inhibited by substrate >50 m*M* H_2O_2. In comparison to BLC, the catalase from the 2P01AA strain was ~3-fold more active at 30 m*M* H_2O_2 in 100 m*M* NaCl. The catalase was also more tolerant toward NaCl concentration, as moderate activity at 200 m*M* NaCl was detected, while BLC displayed irreproducible rates. The catalase was moderately thermostable, where slight, but reproducible, activities were measured at 60°C, whereas for BLC the activity is abolished at 62°C (Switala *et al.*, 1999). The catalase was also very pH stable with no measurable loss in activity between pH 5 and 11.5. Thus, our combined characterizations support the purification of small-subunit, extremely pH stable, alkali-tolerant, halotolerant, and moderately thermostable catalase.

Together, these properties are consistent with the survival features of *A. gyllenbergii* 2P01AA, which is extremotolerant toward H_2O_2 and was isolated from the oligotrophic and low-humidity spacecraft assembly facilities. Survival studies in nutrient-rich media show that *A. gyllenbergii* 2P01AA displays no loss in survival at 100 m*M* H_2O_2 and only a 2-log reduction in 330 m*M* H_2O_2 (Derecho *et al.*, 2014), which represents perhaps the highest survival against H_2O_2 among Gram-negative and non-spore-forming bacteria (McCoy *et al.*, 2012; Derecho *et al.*, 2014). These trends are consistent with the apparent K_m values, which indicate that sufficient catalase activities would be found within the cell in the presence of 100 and 330 m*M* H_2O_2. For example, the catalase enzyme at these H_2O_2 concentrations would not be saturated and accordingly would degrade H_2O_2 at rates of 30% and 59% of V_{max}—which assumes (A) a relatively high intracellular NaCl concentration of 100 m*M* (Schultz *et al.*, 1962), (B) an apparent K_m of 230 m*M* in 100 m*M* NaCl, and (C) a substantially decreased substrate inactivation/inhibition

in vivo. Relatedly, the extremely high catalase specific activities in extracts of *A. gyllenbergii* 2P01AA (1800 ± 350 Units/mg) (Derecho *et al.*, 2014) are likely due to the high apparent k_{cat} and k_{cat}/K_m values, and not necessarily due to high catalase abundances, as changes in catalase volumes upon H_2O_2 exposure have yet to be detected by proteomics. Further, initial experiments showed that cultures of spacecraft-associated *Acinetobacter* grown in nutrient-rich and nutrient-limited media possess similar total catalase specific activities, which suggests that the expression of catalase is relatively independent of carbon nutrient content (unpublished results). Thus, the measured alkali-tolerance of catalase is potentially significant, as *A. gyllenbergii* 2P01AA was initially retrieved from the floor of the Mars Phoenix assembly facility, which was routinely cleaned with alkaline detergents, and subsequently isolated on R2A agar plates, which were adjusted to pH 11 (Vaishampayan *et al.*, 2010; Derecho *et al.*, 2014). Further, the halotolerance and increase in K_m under high salt concentrations are consistent with survival in low-humidity environments (Potts, 1994) and thereby potentially relate to survival in the low-humidity assembly facilities.

5. Conclusion

In conclusion, our work reveals that the catalase kinetic and stability properties are consistent with molecular adaptations toward the alkaline, low-humidity, and potentially oxidizing conditions of the spacecraft assembly facilities (NASA-KSC, 1999; Vaishampayan *et al.*, 2012; Derecho *et al.*, 2014). To date, there remain very few reports that focus on the proteomic underpinnings of the extremotolerance of spacecraft-associated microorganisms (Checinska *et al.*, 2012; McCoy *et al.*, 2012; Derecho *et al.*, 2014). Hence, this study reveals key enzymatic details into the survival of *A. gyllenbergii* 2P01AA and represents perhaps the first purification and characterization of a protein from a spacecraft-associated microorganism. Thus, our collective results support the hypothesis that the selective pressures of the spacecraft assembly conditions impact the microbial communities at the molecular level, which may have broad implications for future life-detection missions.

Acknowledgments

This work was funded by the NASA Astrobiology Institute Minority Institutional Research Support award (R. Mogul) and in part by the Chemistry and Biochemistry Department of Cal Poly Pomona. We also thank the industrial partners of Cal Poly Pomona for access to analytical instrumentation.

References

Allgood, G. and Perry, J. (1986) Characterization of a manganese-containing catalase from the obligate thermophile *Thermoleophilum album*. *J Bacteriol* 168:563–567.

Arnold, K., Bordoli, L., Kopp, J., and Schwede, T. (2006) The SWISS-MODEL workspace: a web-based environment for protein structure homology modelling. *Bioinformatics* 22:195–201.

Benkert, P., Biasini, M., and Schwede, T. (2011) Toward the estimation of the absolute quality of individual protein structure models. *Bioinformatics* 27:343–350.

Biasini, M., Bienert, S., Waterhouse, A., Arnold, K., Studer, G., Schmidt, T., Kiefer, F., Cassarino, T.G., Bertoni, M., Bordoli, L., and Schwede, T. (2014) SWISS-MODEL: modelling protein tertiary and quaternary structure using evolutionary information. *Nucleic Acids Res* 42:W252–W258.

Castro, V.A., Thrasher, A.N., Healy, M., Ott, C.M., and Pierson, D.L. (2004) Microbial characterization during the early habitation of the International Space Station. *Microb Ecol* 47:119–126.

Checinska, A., Burbank, M., and Paszczynski, A.J. (2012) Protection of *Bacillus pumilus* spores by catalases. *Appl Environ Microbiol* 78:6413–6422.

Daly, M.J. (2009) A new perspective on radiation resistance based on *Deinococcus radiodurans*. *Nat Rev Microbiol* 7: 237–245.

Deisseroth, A. and Dounce, A.L. (1970) Catalase: physical and chemical properties, mechanism of catalysis, and physiological role. *Physiol Rev* 50:319–375.

Derecho, I., McCoy, K.B., Vaishampayan, P., Venkateswaran, K., and Mogul, R. (2014) Characterization of hydrogen peroxide-resistant *Acinetobacter* species isolated during the Mars Phoenix spacecraft assembly. *Astrobiology* 14:837–847.

Esaka, M. and Asahi, T. (1982) Purification and properties of catalase from sweet potato root microbodies. *Plant Cell Physiol* 23:315–322.

Frick, A., Mogul, R., Stabekis, P., Conley, C.A., and Ehrenfreund, P. (2014) Overview of current capabilities and research and technology developments for planetary protection. *Adv Space Res* 54:221–240.

Fu, X., Wang, W., Hao, J., Zhu, X., and Sun, M. (2014) Purification and characterization of catalase from marine bacterium *Acinetobacter* sp. YS0810. *Biomed Res Int* 474, doi:10.1155/2014/409626.

Gerischer, U. (2008) Acinetobacter *Molecular Microbiology*, Caister Academic Press, Norfolk, UK.

Ghosh, S., Osman, S., Vaishampayan, P., and Venkateswaran, K. (2010) Recurrent isolation of extremotolerant bacteria from the clean room where Phoenix spacecraft components were assembled. *Astrobiology* 10:325–335.

Gioia, J., Yerrapragada, S., Qin, X., Jiang, H., Igboeli, O.C., Muzny, D., Dugan-Rocha, S., Ding, Y., Hawes, A., Liu, W., Perez, L., Kovar, C., Dinh, H., Lee, S., Nazareth, L., Blyth, P., Holder, M., Buhay, C., Tirumalai, M.R., Liu, Y., Dasgupta, I., Bokhetache, L., Fujita, M., Karouia, F., Eswara Moorthy, P., Siefert, J., Uzman, A., Buzumbo, P., Verma, A., Zwiya, H., McWilliams, B.D., Olowu, A., Clinkenbeard, K.D., Newcombe, D., Golebiewski, L., Petrosino, J.F., Nicholson, W.L., Fox, G.E., Venkateswaran, K., Highlander, S.K., and Weinstock, G.M. (2007) Paradoxical DNA repair and peroxide resistance gene conservation in *Bacillus pumilus* SAFR-032. *PLoS One* 2:e928.

La Duc, M.T., Nicholson, W., Kern, R., and Venkateswaran, K. (2003) Microbial characterization of the Mars Odyssey spacecraft and its encapsulation facility. *Environ Microbiol* 5:977–985.

La Duc, M.T., Kern, R., and Venkateswaran, K. (2004a) Microbial monitoring of spacecraft and associated environments. *Microb Ecol* 47:150–158.

La Duc, M.T., Satomi, M., and Venkateswaran, K. (2004b) *Bacillus odysseyi* sp. nov., a round-spore-forming bacillus isolated from the Mars Odyssey spacecraft. *Int J Syst Evol Microbiol* 54:195–201.

La Duc, M.T., Vaishampayan, P., Nilsson, H.R., Torok, T., and Venkateswaran, K. (2012) Pyrosequencing-derived bacterial,

archaeal, and fungal diversity of spacecraft hardware destined for Mars. *Appl Environ Microbiol* 78:5912–5922.

Loo, S. and Erman, J.E. (1975) Kinetic study of the reaction between cytochrome c peroxidase and hydrogen peroxide. Dependence on pH and ionic strength. *Biochemistry* 14:3467–3470.

Luo, L., Carson, J.D., Dhanak, D., Jackson, J.R., Huang, P.S., Lee, Y., Sakowicz, R., and Copeland, R.A. (2004) Mechanism of inhibition of human KSP by monastrol: insights from kinetic analysis and the effect of ionic strength on KSP inhibition. *Biochemistry* 43:15258–15266.

McCoy, K., Derecho, I., Wong, T., Tran, H., Huynh, T., La Duc, M., Venkateswaran, K., and Mogul, R. (2012) Insights into the extremotolerance of *Acinetobacter radioresistens* 50v1, a Gram-negative bacterium isolated from the Mars Odyssey spacecraft. *Astrobiology* 12:854–862.

Mogul, R. and Holman, T.R. (2001) Inhibition studies of soybean and human 15-lipoxygenases with long-chain alkenyl sulfate substrates. *Biochemistry* 40:4391–4397.

Moissl-Eichinger, C., Pukall, R., Probst, A.J., Stieglmeier, M., Schwendner, P., Mora, M., Barczyk, S., Bohmeier, M., and Rettberg, P. (2013) Lessons learned from the microbial analysis of the Herschel spacecraft during assembly, integration, and test operations. *Astrobiology* 13:1125–1139.

Nakamura, S. and Kimura, T. (1971) Studies on spinach ferredoxin-nicotinamide adenine dinucleotide phosphate reductase. Kinetic studies on the interactions of the reductase and ferredoxin and a possible regulation of enzyme activities by ionic strength. *J Biol Chem* 246:6235–6241.

NASA-KSC. (1999) Launch Site Requirement Planning Group. In *Facilities Handbook of Payload Hazardous Servicing Facility (PHSF)*, NASA, Cape Canaveral, FL.

Obinger, C., Regelsberger, G., Strasser, G., Burner, U., and Peschek, G. (1997) Purification and characterization of a homodimeric catalase-peroxidase from the cyanobacterium *Anacystis nidulans*. *Biochem Biophys Res Commun* 235:545–552.

Potts, M. (1994) Desiccation tolerance of prokaryotes. *Microbiol Rev* 58:755–805.

Schultz, S.G., Wilson, N.L., and Epstein, W. (1962) Cation transport in *Escherichia coli* II. Intracellular chloride concentration. *J Gen Physiol* 46:159–166.

Space Studies Board. (2006) *Preventing the Forward Contamination of Mars*, National Academies Press, Washington, DC.

Switala, J. and Loewen, P.C. (2002) Diversity of properties among catalases. *Arch Biochem Biophys* 401:145–154.

Switala, J., O'Neil, J.O., and Loewen, P.C. (1999) Catalase HPII from *Escherichia coli* exhibits enhanced resistance to denaturation. *Biochemistry* 38:3895–3901.

Thompson, V.S., Schaller, K.D., and Apel, W.A. (2003) Purification and characterization of a novel thermo-alkali-stable catalase from *Thermus brockianus*. *Biotechnol Prog* 19:1292–1299.

Vaishampayan, P., Osman, S., Andersen, G., and Venkateswaran, K. (2010) High-density 16S microarray and clone library–based microbial community composition of the Phoenix spacecraft assembly clean room. *Astrobiology* 10:499–508.

Vaishampayan, P., Probst, A.J., La Duc, M.T., Bargoma, E., Benardini, J.N., Andersen, G.L., and Venkateswaran, K. (2012) New perspectives on viable microbial communities in low-biomass cleanroom environments. *ISME J* 7:312–324.

von Ossowski, I., Mulvey, M.R., Leco, P., Borys, A., and Loewen, P. (1991) Nucleotide sequence of *Escherichia coli* katE, which encodes catalase HPII. *J Bacteriol* 173:514–520.

Yumoto, I.I., Iwata, H., Sawabe, T., Ueno, K., Ichise, N., Matsuyama, H., Okuyama, H., and Kawasaki, K. (1999) Characterization of a facultatively psychrophilic bacterium, *Vibrio rumoiensis* sp. nov., that exhibits high catalase activity. *Appl Environ Microbiol* 65:67–72.

Address correspondence to:
Rakesh Mogul
California State Polytechnic University
Pomona Chemistry & Biochemistry Department
3801 W. Temple Ave.
Pomona, CA 91768

E-mail: rmogul@csupomona.edu

Submitted 10 October 2014
Accepted 12 January 2015

Abbreviations Used

BLC = bovine liver catalase
HIC = hydrophobic interaction chromatography
LB = lysogeny broth
LC-MS/MS = liquid chromatography–tandem mass spectrometry
OTUs = operational taxonomic units
PBS = phosphate-buffered saline
RT = room temperature
se = standard error
SEC = size-exclusion chromatography